Monthly Notices
of the
ROYAL ASTRONOMICAL SOCIETY

Mon. Not. R. Astron. Soc. **415,** 1355–1365 (2011) doi:10.1111/j.1365-2966.2011.18780.x

Early-type stars in the open cluster NGC 4852

J. A. Ahumada,[1⋆]† E. E. Giorgi,[2⋆]‡ G. Solivella[2⋆]‡ and R. A. Vázquez[2⋆]‡

[1]*Observatorio Astronómico, Universidad Nacional de Córdoba, Laprida 854, 5000 Córdoba, Argentina*
[2]*Facultad de Ciencias Astronómicas y Geofísicas, Universidad Nacional de La Plata, IALP-CONICET, Paseo del Bosque s/n, 1900 La Plata, Argentina*

Accepted 2011 March 24. Received 2011 March 24; in original form 2010 October 6

ABSTRACT

The southern open cluster NGC 4852 was re-observed in the *UBVRI* passbands to refine its intrinsic fundamental parameters. An extended spectral coverage was also undertaken aimed at obtaining a clear picture of the kind of stars inhabiting the cluster upper main sequence. We detected an unusual number of B-type stars including a new weak-emission Be star that raises to three the number of confirmed emission objects known in the cluster area. Our analysis, however, is conclusive in that none of them belongs to the cluster. With the new data set, we improved the fundamental parameters of NGC 4852: it is little bit farther than formerly assumed; the reddening, which increases smoothly with the distance, is lower than early estimates; and more importantly, it is really a young object of nearly 40–60 Myr, contrary to the age of 200 Myr stated before. By means of spectroscopic parallaxes we secured the star distances, finding a good agreement between spectroscopic and zero-age main-sequence fitting distances, within the errors. The spatial distribution of the stars allows us to infer that NGC 4852 is the final, closer to the Sun, structure of a star-forming region and that a distant group of early-B-type stars, located immediately beyond the cluster, seems to be part of an extended OB association. The three emission stars detected in the region are related to this farther group. Finally, two extremely faint and blue stars were also found in the cluster zone. They have no connection with NGC 4852 but seem to be white-dwarf candidates.

Key words: stars: early-type – stars: emission-line, Be – open clusters and associations: general – open clusters and associations: individual: NGC 4852 – Galaxy: structure.

1 INTRODUCTION

NGC 4852 (C1257−593) is a moderately compact open cluster that lies in Centaurus, at $l = 304\overset{\circ}{.}03$, $b = +3\overset{\circ}{.}24$ ($\alpha = 13^{\rm h}00\overset{\rm m}{.}1$, $\delta = -59^{\circ}36\overset{'}{.}7$, J2000.0). In the neighbourhood of this location, not far from the Coalsack nebula, there are the prominent and extensively studied cluster NGC 4755 (at $\sim 1\overset{\circ}{.}1$) and the much less known cluster Loden 694 (at $\sim 1\overset{\circ}{.}4$). NGC 4852 has a Trumpler class I3c and an apparent diameter of 12 arcmin according to Lyngå (1987).

Recently, Carraro et al. (2005) carried out a deep and extensive *UBVI* photometric survey in the area of NGC 4852 down to $V =$ 22–23 mag using the ESO Wide Field Imager, an array of eight CCDs that covers a field of approximately 34×33 arcmin^2. Due to the strategy followed by these authors, a number of stars brighter than $V = 12$ were not being measured because of saturation. The authors were nevertheless able to set the parameters of NGC 4852, placing it at 1.1 kpc from the Sun, adopting a mean colour excess $E(B-V) = 0.45$ (given by visual inspection) and estimating its age to be in the range 200–250 Myr.

As reported in the literature, in the cluster area, there are two emission stars: Wray 15-1039 (Wackerling 1970; Stephenson & Sanduleak 1977) and CPD −59 4639, a Be star (Feast, Thackeray & Wesselink 1957). The nearby cluster NGC 4755, a fairly young object (10–14 Myr, Sagar & Cannon 1995; Bonatto et al. 2006), also has emission stars. Although it remains a difficult astrophysical problem to confirm if the Be phenomenon is an evolutionary effect happening in the second half of the main-sequence lifetime, or if it originates in the conditions of the formation of some stars, which include fast rotation and probably other factors (Fabregat & Torrejón 2000), it seems to be clearly established that this emission phase shows a high-frequency peak in clusters about 13–25 Myr old (Fabregat & Torrejón 2000). It is also well known that Be-type stars are hardly observed in clusters older than 100 Myr (McSwain & Gies 2005). We therefore wonder if the loss of the brightest and earliest cluster members in the Carraro et al. study led them to assume for NGC 4852 an incorrect older age, since the presence of

⋆E-mail: javier@oac.uncor.edu (JAA); egiorgi@fcaglp.unlp.edu.ar (EEG); gladys@fcaglp.unlp.edu.ar (GS); rvazquez@fcaglp.unlp.edu.ar (RAV).
†Visiting Astronomer, Cerro Tololo Inter-American Observatory (CTIO), operated by the AURA, Inc., under contract to the National Science Foundation.
‡Visiting Astronomer, Complejo Astronómico El Leoncito (CASLEO), operated under agreement between the Consejo Nacional de Investigaciones Científicas y Técnicas de la República Argentina and the National Universities of La Plata, Córdoba and San Juan.

emission stars (in particular, of Be type) in the cluster area suggests a priori that it is a young cluster rather than an intermediate-age one, as they proposed. In this work, we want to scrutinize the upper main sequence of the cluster to clearly state its fundamental parameters and to study its possible connection with the mentioned emission stars.

Bearing this in mind, we undertook a vigorous effort to obtain spectroscopy for 40 of the brightest stars of NGC 4852, as well as *UBVRI* photometry of the very centre of the cluster. Besides our wish to clarify the evolutionary status of this object and to refine its parameters, we also aim at a better interpretation of the role of emission stars in open clusters. This is an issue of major astrophysical interest as pointed out by McSwain & Gies (2005) whose results indicate, additionally, a possible increase in the fraction of Be stars with increasing Galactocentric distance (in environments of decreasing metallicity), a question that remains open due to the scatter in their data.

Just for the sake of completeness, and in terms of what is known about NGC 4852, we want to mention that Carraro et al. (2005) also derived luminosity functions and present-day mass functions (MFs), finding that the cluster is one of the most extended in mass and that its MF slope is basically consistent with the classical Salpeter (1955) MF over the whole mass range, that is, there is no any significant change in slope. According to Scalo (1998), the mean slope for the MF in clusters younger than half a Gyr is $x = 2.25 \pm 0.88$ and the MF of NGC 4852 reflects this behaviour. Therefore, this is another reason to set on a firmer base the parameters of the cluster.

2 PHOTOMETRIC DATA

The field of NGC 4852 was observed at the Cerro Tololo Inter-American Observatory (CTIO, Chile) with the 1-m (ex YALO, now operated by the SMARTS Consortium) telescope and the Y4K Camera[1] (Y4KCam) of the Ohio State University. The Y4KCam has a 4K×4K CCD that covers a square on the sky of $20 \times 20\,\mathrm{arcmin}^2$ at a scale of 0.289 arcsec pixel^{-1}; the filters provided include a Johnson–Cousins *BVRI* set plus a $U+$ $CuSO_4$ filter.

The observing procedure was as follows. To eliminate cosmic rays and improve the signal-to-noise ratio, three identical exposures per filter were taken and combined; the full reduction was performed on these combined images. Short exposures to measure bright stars were also taken. The cluster was observed on two nights (2006 April 22–23 and 23–24, of a three-night observing run) to cross-check the internal consistency of the photometry and combine the data wherever possible. Details pertinent to the observations are in Table 1. Sky flats (U filter) and dome flats (*BVRI* filters) were obtained and used. The dome flat illumination coincides acceptably with that of the sky flat on an area of ∼2K × 2K around the position $(x, y) = (1500, 1500)$, but, outside it, they depart increasingly; for this reason, the cluster was centred around the mentioned position, resulting in an area for our survey of $11.1 \times 11.6\,\mathrm{arcmin}^2$.

To do absolute photometry, more than 30 standard stars of Graham (1982) were observed throughout each night of the run; the stars belong to Graham's E4–E8 fields. The range in the index $(B - V)$ for the observed standard stars was 0.02–1.32, that for $(U - B)$ was −0.42 to 1.41, that for V was 9.3–16.5 and the range of the airmass covered was 1.04–1.30.

[1] http://www.astronomy.ohio-state.edu/Y4KCam/

Table 1. Log of observations.

Night	Filter	Exposure time (s)	UT[a] (h m)	FWHM[b] (arcsec)	Airmass[c]
2006 April 22–23	*B*	120	3 35	1.5	1.15
	V	60	3 49	1.3	1.15
	R	40	3 57	1.4	1.15
	I	40	4 05	1.4	1.15
	U	100	4 15	1.7	1.16
2006 April 23–24	*B*	120	5 13	1.6	1.21
	V	60	5 25	2.1	1.22
	R	40	5 33	1.6	1.23
	I	40	5 41	1.4	1.24
	U	100	5 52	1.9	1.26

[a]Time in the middle of the second exposure.
[b]Full width at half-maximum: mean value of the combined images.
[c]Airmass of the middle of the second exposure.

The reduction and photometric procedures were mostly carried out inside the IRAF[2] environment. Although the frames were processed as usual, the images of the Y4KCam required an additional step since, to avoid a high readout time, the chip's four quadrants are read independently and thus have different levels of bias. Following the procedure suggested by P. Massey[3] and using his programs, each raw image was first cut into four quadrants, each part was then corrected by the corresponding overscan, and lastly the quadrants were rejoined to continue the processing of the entire image. The differences among the quadrants were nevertheless impossible to eliminate completely; in our typical, long-exposure, fully reduced V frames, the jumps were of about 30 ADUs, not significant for the purposes of this work.

The photometric package utilized was DAOPHOT (Stetson 1987, 1990). Aperture photometry was performed to obtain the instrumental magnitudes of standard stars and some bright cluster stars. Profile-fitting photometry was performed in each program frame by constructing the corresponding point spread function. The zero-point of the instrumental magnitudes for each image was determined with small-aperture photometry and growth curves.

For each of the three nights, the transformation coefficients were of the form

$$M = m + c_0 + c_1 \times X + c_2 \times C, \quad (1)$$

where M and m are the standard and instrumental magnitudes, X is the airmass, C is an appropriate standard colour index and c_i are the zero-point, first-order extinction, colour-term coefficients. A second-order extinction term did not seem to improve the fittings. The C indices are $(B - V)$ for U, B and V; $(V - R)$ for R; and $(R - I)$ for I. The nightly c_i coefficients were averaged and are listed in Table 2. The mean rms errors of the individual transformations are 0.027 (U), 0.022 (B), 0.020 (V), 0.022 (R) and 0.022 mag (I). An inspection of Table 2 shows in particular that the colour term for B has rather a large negative value, which indicates that the provided B filter is non-standard. Unfortunately, there are few B stars in the Graham list of stars to trace out the effect of this non-standard filter on the U and B magnitudes for B stars, so it is not feasible to fit a different transformation for $(U - B)$ and $(B - V)$ for the bluest stars (as pointed out by Graham 1982). Therefore, it is likely that

[2] IRAF is distributed by the National Optical Astronomy Observatories which are operated by the Association of Universities for Research in Astronomy, Inc., under cooperative agreement with the National Science Foundation.
[3] http://www.lowell.edu/users/massey/obins/y4kcamred.html

Table 2. Mean coefficients of the transformation equations.

Mag	c_0	σ	c_1	σ	c_2	σ
U	+0.95	0.07	−0.53	0.05	+0.01	0.01
B	+2.18	0.06	−0.39	0.05	−0.17	0.01
V	+2.06	0.05	−0.10	0.05	+0.02	0.01
R	+2.12	0.08	−0.10	0.05	+0.05	0.02
I	+1.31	0.05	−0.06	0.04	+0.04	0.02

the *UBV* colours of the bluest and earliest spectral-type stars in the field of NGC 4852 are not as well standardized as stars later than B8.

As for the program stars, no general trends were noted when the photometric data of both nights were compared, so they were combined in one single list of magnitudes and colours. The final photometry for NGC 4852 is in Table 3 and consists of 3334 entries. Fig. 1 is the finding chart (enclosed by a short-dashed square) superposed to a DSS blue plate.

The five stars numbered from #10001 to #10005 in Fig. 1 and listed at the end of Table 3 deserve a comment. The bright stars #10001 (HD 112852) and #10003 are in the field observed at the CTIO, but they could not be measured because of saturation; the other three stars are outside the observed region. Since it was desirable to have photometry of these stars as they are included in our spectroscopic survey (see the next section), additional measurements of the cluster in the form of very short exposures in *UBV* were carried out using the 1340 × 1300 Roper CCD[4] attached to the 2.15-m telescope at the Complejo Astronómico El Leoncito (CASLEO), Argentina. These data were calibrated using stars already observed at the CTIO as secondary standards. Technical details and reduction procedures for Roper CCD observations, including typical extinction coefficients, can be found in Giorgi et al. (2007).

Fig. 2 shows five panels where the errors in colours and magnitudes returned by DAOPHOT are indicated as a function of *V*. Down to $V \simeq 19$ mag all stars have low errors except for the $(U - B)$ index, which strongly increases for larger *V* magnitudes. This is the result of relatively short exposure times. We compared our photometry with that of Carraro et al. (2005); mean differences (in the sense: this paper *minus* Carraro et al.) and standard deviations were computed at two apparent magnitude levels as shown in Table 4. The number of stars *N* involved in each determination is also indicated. The agreement in *V* is reasonably good at any *V* magnitude limit, the mean difference in $(B - V)$ is rather large and the scatter around the mean seems to be important only at fainter magnitudes. In the case of $(U - B)$, the mean differences are not significant, but the standard deviations are, on the contrary, quite large in both apparent magnitude limits.

3 SPECTROSCOPIC DATA

Low-resolution spectra were obtained for 40 stars distributed across the cluster surface in 2005 February and March, 2006 July, 2007 March and 2010 April at the CASLEO. The instrument utilized was a spectrograph REOSC[5] in simple dispersion mode attached to the Cassegrain focus of the 2.15-m telescope, using a 600 l mm^{-1} grating in the first order with a dispersion of 1.64 Å pixel^{-1}, and a CCD Tek 1024 × 1024 detector. The spectra achieved a signal-to-noise ratio of about 200 and cover a wavelength range that goes from 3800 to 6200 Å, that is, from the Ca II K and H lines to beyond Hβ, the spectral region traditionally used in the MK classification for the determination of accurate spectral types. The reduction process was carried out with standard procedures and routines running within IRAF.

For classification purposes, MK standard stars were also observed with the same configuration at the CASLEO, and the Digital Spectra Classification of R. O. Gray[6] and the MK Standard[7] were used. An estimate of the accuracy of our classification indicates that, potentially, it can be wrong in half a subtype and one luminosity class with reference to the classification scheme (see, however, Section 5). The normalized spectra are shown in Fig. 3 along with the corresponding star identifications and MK classifications. Table 5 lists the derived spectral types for the 40 stars, together with the apparent magnitudes, colour excesses, absolute magnitudes, apparent distance moduli and distances (with their errors) obtained from the MK classifications; a further discussion of these spectra is in Section 5.

4 REVISING THE CLUSTER PARAMETERS: PHOTOMETRY AND SPECTROSCOPY

4.1 Cluster size

The apparent size of NGC 4852 was carefully determined through star counts by Carraro et al. (2005) who indicated that the cluster radius is about 4 arcmin when counts include all stars down to $V = 16$. This value is similar to the one found by Ahumada (2008) in a preliminary analysis of the photometric data of Section 2, by comparing the cluster colour–magnitude diagrams with those of a nearby field. However, the very deep photometry of Carraro et al. also shows that the cluster radius increases up to 6 arcmin at magnitudes ranging from $V = 16$ to 18; after that limit, the cluster vanishes into the stellar background. The present photometric survey therefore includes the entire cluster down to $V = 16$ and about 90 per cent of the cluster below this magnitude.

4.2 Reddening towards the cluster

Given the evident youth of the cluster (see diagrams in Fig. 6 shown later), there are a number of early-type stars that can be used to estimate the cluster reddening by means of the well-known *Q*-method, that is, solving the equations $Q = (U - B) - x \times (B - V)$, $x = 0.72 + 0.05 \times E(B - V)$ and $(B - V)_0 = 0.332 \times Q$ using iterations. The requirement of an approximately linear relation between $(U - B)$ and $(B - V)$ in the colour–colour diagram (upper left-hand panel in Fig. 6 shown later) suggests that stars with observed $(B - V)$ lesser than ∼0.36 be used in the iterations; besides, the group of bright stars that clearly appear detached from the sequence in the same diagram (see discussion in Section 4.4) puts an upper limit of $(U - B) \sim -0.3$, thus leaving a total of 21 stars to calculate the reddenings. In this way, we obtain $E(B - V) = 0.36 \pm 0.01$ and $E(U - B) = 0.27 \pm 0.01$.

[4] http://www.casleo.gov.ar/instrumental/js-ccdd.html
[5] http://www.casleo.gov.ar/instrumental/js-reosc.html
[6] http://nedwww.ipaccaltech.edu/level5/Gray
[7] http://stellar.phys.appstate.edu/Standards

Table 3. Photometry of NGC 4852.[a]

Star Id	Xcoo	Ycoo	V	$\epsilon(V)$	$B-V$	$\epsilon(B-V)$	$U-B$	$\epsilon(U-B)$	$V-I$	$\epsilon(V-I)$	$V-R$	$\epsilon(V-R)$
1	−435.21	−928.60	9.733	0.001	0.276	0.001	−0.541	0.001	–	–	–	–
2	+790.76	−685.66	10.104	0.001	0.551	0.001	0.167	0.004	–	–	–	–
3	−995.13	+161.55	10.379	0.001	0.206	0.001	−0.526	0.001	0.387	0.001	0.173	0.001
4	+318.97	+117.70	10.473	0.001	0.194	0.001	−0.291	0.001	0.321	0.002	0.123	0.001
5	+770.53	+763.81	10.619	0.001	0.188	0.001	−0.189	0.002	0.344	0.002	0.142	0.001

[a]This table is available in full with the online version of the article (see Supporting Information). A portion is shown here for guidance regarding its form and content.

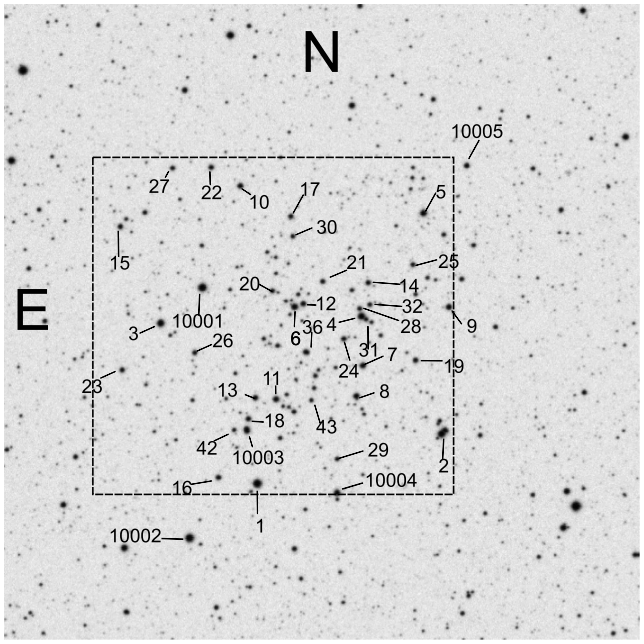

Figure 1. Finding chart of NGC 4852 adapted from a DSS plate. The dashed square approximately delimits the area covered by our photometry. Stars analysed spectroscopically are numbered.

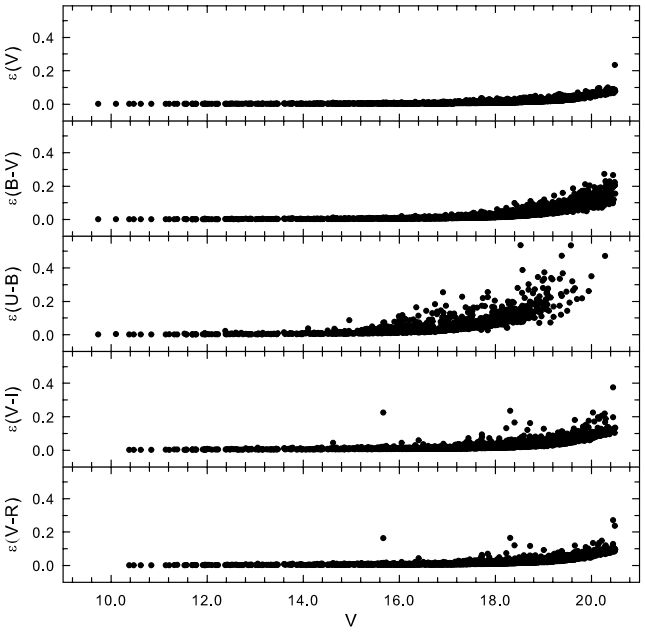

Figure 2. Errors returned by DAOPHOT as a function of the V magnitude.

Table 4. Mean differences with Carraro et al. (2005).

V limit	$\Delta(V)$	σ	$\Delta(B-V)$	σ	$\Delta(U-B)$	σ	N
<18	0.00	0.02	−0.11	0.05	+0.02	0.12	450
<20	0.00	0.04	−0.11	0.11	−0.02	0.13	1234

4.3 Extinction towards the cluster

We start by inspecting the colour-excess relation that can be used to estimate intrinsic colours, taking advantage of the large number of available spectral types. In Fig. 4, we plot the reddenings $E(U-B)$ and $E(B-V)$ derived from the individual spectral types, luminosity classes and intrinsic colour indices given by Schmidt-Kaler (1982) and listed in Table 5 (columns 4 and 5). The solid line is the canonical relation $E(U-B) = 0.72 \times E(B-V) + 0.05 \times E(B-V)^2$. Two facts preclude us from estimating the precise value of the colour-excess relation in the cluster: the most important one is that the reddening range is too small to perform a reliable fitting of the data; the other is the presence of some spread in the colour excesses produced partly by cosmic data scatter, but mainly because of the uncertainties in our classification.

Therefore, we assume that the canonical law is fully representative of the colour-excess relation across NGC 4852.

The next step is to combine our photometry with 2MASS data (Skrutskie et al. 2006) and with our spectral classification of 40 stars (Section 3) to estimate the value of the ratio $R = A_V/E(B-V)$. For this, we applied the colour-difference method based on the van der Hulst # 15 extinction curve (Johnson 1968), which computes the colour excesses in visible and infrared wavelengths. As above, in the visible range, we combined our data with intrinsic colours and spectral types from Schmidt-Kaler (1982); in the infrared, we used analogous relations from Koornneef (1983) combined with *JHK* 2MASS data. All the individual colour excesses $E(U-V)$, $E(V-R)$, $E(V-I)$, $E(V-H)$, $E(V-J)$ and $E(V-K)$ were normalized to $E(B-V) = 1$ and averaged to allow the comparison with the curve # 15, for which $E(U-V)/E(B-V) = 1.70$, $E(V-R)/E(B-V) = 0.70$, $E(V-I)/E(B-V) = 1.24$, $E(V-H)/E(B-V) = 2.30$, $E(V-J)/E(B-V) = 2.70$ and $E(V-K)/E(B-V) = 2.90$, as given in Johnson (1968) and rectified for Cousins passbands.

Fig. 5 shows the observed mean curve (dashed line) from our stars plotted in the $E(X-V)/E(B-V)$ versus λ^{-1} plane, together with the curve # 15. The vertical bars stand for the standard deviation of the mean at each wavelength. According to the usual procedure, the asymptotic projection of the mean observed curve to infinite wavelength gives the ratio of visual to selective absorption, R. We can see that the mean observed values are almost coincident with the curve # 15 along the full range of wavelength. The slight departure of the observed curve with respect to curve # 15 is produced by the

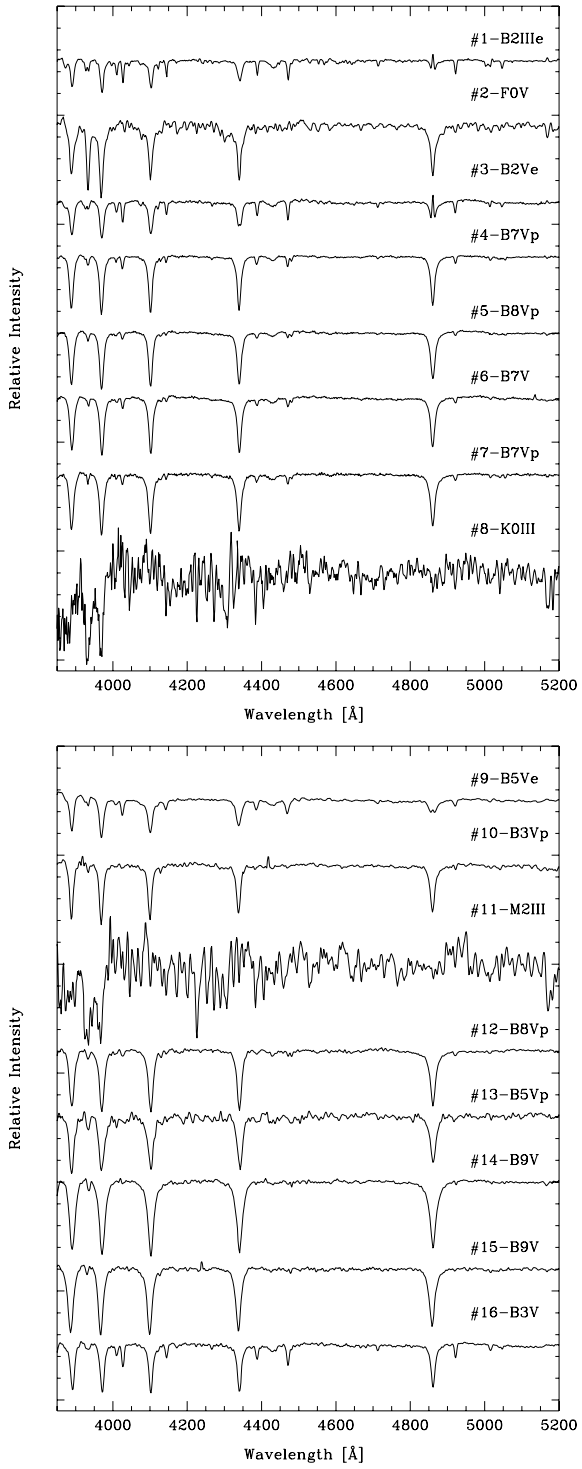

Figure 3. Normalized spectra and spectral classifications for 40 stars in NGC 4852. Star identifications and spectral types are shown.

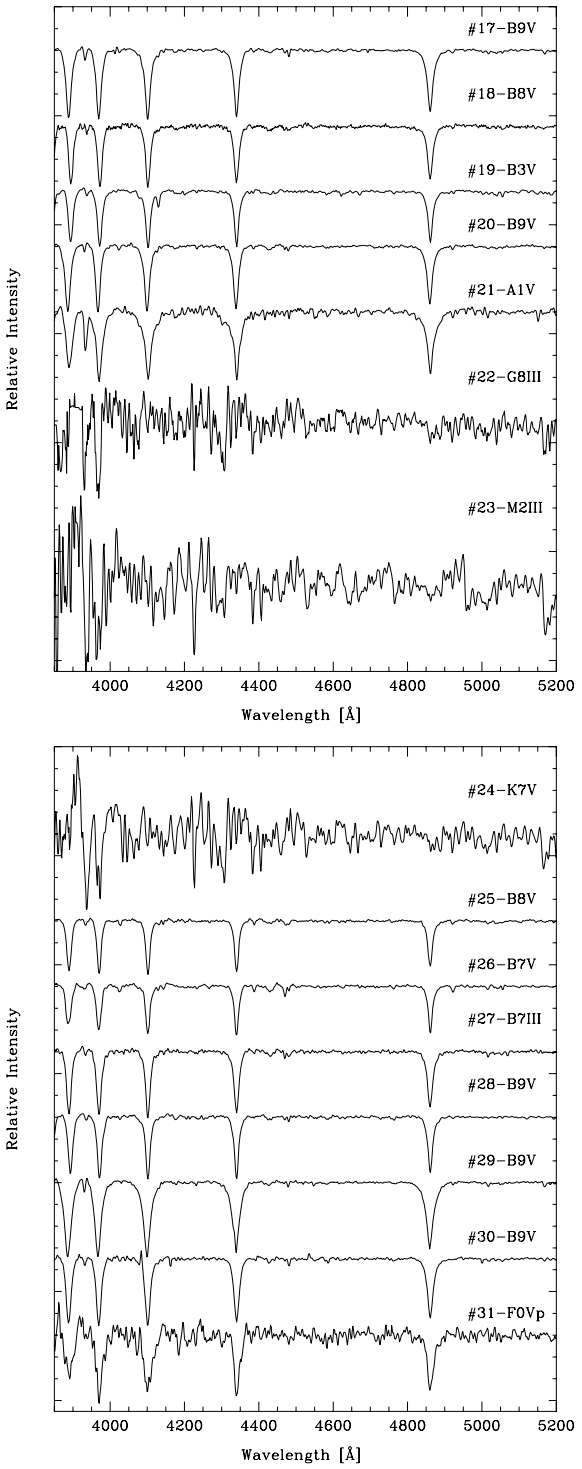

Figure 3 – *continued*

influence of a few stars with anomalous infrared colours. Exceptions aside, the mean observed curve tends asymptotically to the normal value $R = 3.1$, which we therefore adopt for NGC 4852.

4.4 Colour–colour and colour–magnitude diagrams

Prior to building the photometric diagrams, we discarded those stars with photometric errors larger than 0.10 mag to reduce noise and to increase the quality of the diagrams, especially towards fainter magnitudes. This is a reasonable procedure that, although diminishing the number of stars available at the low-luminosity part of the diagrams, nevertheless reduces the presence of false structures produced by large errors.

Fig. 6 shows four photometric diagrams of NGC 4852. The following comments arise after a brief inspection. The cluster sequence, clearly detached from the general star field, appears in all the panels. Of special interest is the two-colour diagram (TCD,

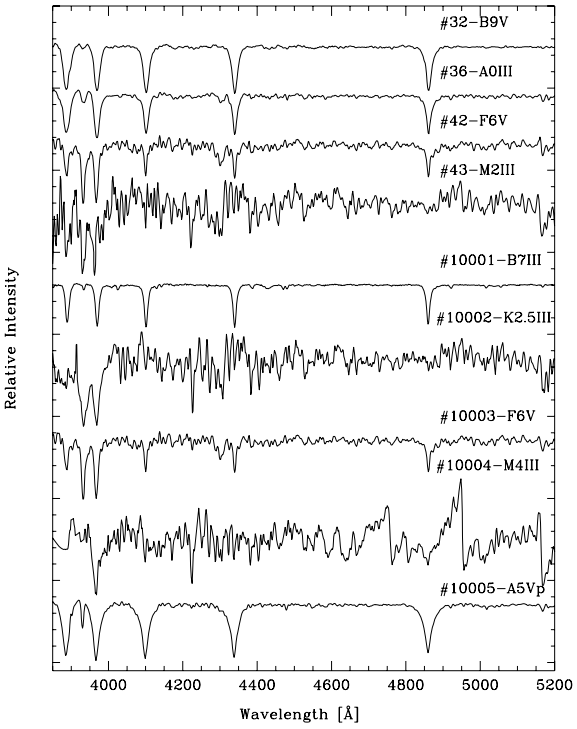

Figure 3 – *continued*

upper left-hand panel), where the stars are shown together with the intrinsic colour–colour line of Schmidt-Kaler (1982). The cluster sequence extends from $(U - B) = -0.60$ down to $(U - B) = +0.40$, showing some scatter among the bluest stars from $-0.60 < (U - B) < -0.10$. Stars that belong to this scattered group are indicated with a (+) in all the panels. Longwards $(B - V) = 0.80$, the cluster sequence merges into another, probably formed by field stars. The entire TCD shows a tail of red stars including probable giants. The zero-age main-sequence (ZAMS, long-dashed line) was shifted the mean colour excesses $E(B - V) = 0.39 \pm 0.03$ and $E(U - B) = 0.28 \pm 0.02$ to fit properly the cluster sequence; the errors were estimated by eye inspection. These reddenings are consistent with those obtained from the photometry (Section 4.2). Carraro et al. (2005), who applied a similar strategy to the same empirical ZAMS, obtained the larger value $E(B - V) = 0.45$. We speculate that the difference may come, first, from the loss of the brightest stars in Carraro et al., which precluded them from considering the obvious data scatter reflected in the TCD, and, secondly, from the difference between the $(B - V)$ indices in both photometries (cf. Table 4).

Turning to the stars represented by a (+), it is interesting to see how clearly they detach from the rest in the V versus $(U - B)$ diagram (lower left-hand panel), composing a parallel sequence of stars located beyond the cluster and not related to it. It should be recalled here that the $(U - B)$ index is a powerful tool because it is a better temperature discriminator and it is sensitive to reddening effects; for this reason, the pattern is not visible in the remaining colour–magnitude diagrams. However, not all of these stars are located behind NGC 4852: two of them, # 925 and # 943, are very blue and extremely faint, which makes them serious candidates to become white dwarf stars located somewhere in between the cluster and the Sun.

The spectral classification in Table 5 leaves no doubt about this: the (+) stars have (on average) earlier B spectral types than the stars in NGC 4852. Both groups are seen with similar apparent magnitudes just because the hotter are at larger distances from the Sun. This is the best explanation for what is evident from the V versus $(U - B)$ diagram: eight stars compose a parallel hot sequence of distant stars, of which three are early (B3) Be-type stars and two stars are very faint, hot stars.

The remaining panels in Fig. 6 show a series of stars that have similar reddenings and cooler spectral types, from a photometric perspective. Finally, at $V \sim 16$ the cluster vanishes into a population of thin-disc field stars.

It is worth drawing attention to the clear gap in the main sequence covering a magnitude V range from 13.5 to 13.8 and centred at $(B - V) = 0.5$. At the same apparent magnitude, the gap appears better defined in the V versus $(V - I)$ diagram, but is almost invisible in the V versus $(U - B)$ diagram. Although the analysis of the true nature of this gap is outside the scope of this paper, and we just want to point out to its presence for further research, the following remarks may nevertheless be of interest. According to the cluster distance and reddening derived in this paper, the absolute magnitude of the gap corresponds to absolute magnitudes, M_V, ranging from 1.6 to 1.9, the typical magnitudes of A0–A3 type stars. This location differs from that of other gaps observed in open cluster main sequences, as the hot one for B5–B8 type stars (Mermilliod 1976) or the one for A7–F0.5 type stars (Böhm-Vitense & Canterna 1974). Now, as mentioned in the Introduction, at about 1°.1 from NGC 4852 lies the interesting open cluster NGC 4755. The distance of this young (10 Myr) object is near 2.0 kpc (Sagar & Cannon 1995), which places it at the distance of a farther B-type star group (cf. Section 5) with a similar reddening of 0.41. The Sagar & Cannon photometry leaves no doubt as to the existence of a main-sequence hot gap for M_V in the range from -1.75 to -2.1. Another nearby cluster, Loden 694, a young (24-Myr) object as well and located at 1.7 kpc from the Sun (Kharchenko et al. 2005), also shows a gap in its main sequence, although not very well defined. It should be analysed in a more general context whether it is just a matter of chance to find three clusters with an identical signature or we can relate this high frequency to other factors.

4.5 Distance and age

In this section, we discuss how we derived the cluster distance. We exemplify the procedure in Fig. 7, where the empirical ZAMS of Schmidt-Kaler (1982) has been superposed to the V versus $(B - V)$ and V versus $(U - B)$ diagrams. The ZAMS was shifted the mean cluster reddening and moved vertically to get the best possible fitting by the left envelope of the cluster main sequence. We thus obtained an apparent distance modulus $V - M_V = 11.90 \pm 0.10$ in the V versus $(B - V)$ plane. A similar procedure applied to the V versus $(U - B)$ diagram yields 11.60 ± 0.10 and to the V versus $(V - R)$ and $(V - I)$ diagrams, using the respective intrinsic relations from Cousins (1978), gives 11.90 ± 0.15. In all cases, the error of the fitting was estimated by eye. We adopt the last value as the most probable apparent distance modulus for NGC 4852. After correcting for a visual absorption $A_V = 3.1 \times 0.38 = 1.18$ mag, the distance of the cluster turns out to be 1390^{+70}_{-60} pc, about 200 pc larger than the estimate of Carraro et al. (2005). Since the procedures to get distances in both papers are similar, we conclude, again, that the difference may be the result of the loss (in the Carraro et al. study) of the brightest stars of the cluster.

At the calculated distance and apparent size (Section 4.1), NGC 4852 has a real diameter of at least 5 pc. It is located at a Galactocentric radius of about 7.8 kpc (adopting a value of 8.5 kpc

Table 5. Spectral types in NGC 4852.

Star Id	Spectral type	V	$E(B-V)$	$E(U-B)$	M_V	$V-M_V$	d (pc)	ϵ_d (pc)	Remarks
1	B2IIIe	9.73	0.52	0.37	−3.90	13.63	2551	117	OB
2	F0V	10.10	0.25	0.14	2.70	7.40	211	10	
3	B2Ve	10.38	0.45	0.31	−2.45	12.83	1947	90	OB
4	B7Vp	10.47	0.32	0.14	−0.60	11.07	1032	48	m?
5	B8Vp	10.62	0.30	0.15	−0.25	10.87	975	45	nm
6	B7V	10.84	0.34	0.19	−0.60	11.44	1198	55	m
7	B7Vp	11.14	0.35	0.19	−0.60	11.74	1362	63	m
8	K0III	11.21	0.39	0.56	0.70	10.51	731	34	
9	B5Ve	11.32	0.39	0.13	−1.20	12.52	1821	84	OB
10	B3Vp	11.38	0.53	0.54	−1.60	12.98	1861	86	OB
11	M2III	11.53	0.34	0.42	−0.60	12.13	1642	76	
12	B8Vp	11.57	0.38	0.27	−0.25	11.82	1335	61	m
13	B5Vp	11.58	0.42	0.48	−1.20	12.78	1959	90	OB
14	B9V	11.69	0.31	0.29	0.20	11.49	1269	58	m
15	B9V	11.70	0.40	0.24	0.20	11.50	1130	52	m
16	B3V	11.70	0.48	0.30	−1.60	13.30	2306	106	OB
17	B9V	11.76	0.41	0.27	0.20	11.56	1146	53	m
18	B8V	11.76	0.39	0.27	−0.25	12.01	1445	67	m
19	B3Vp	11.77	0.40	0.47	−1.60	13.37	2667	123	OB
20	B9V	11.91	0.36	0.17	0.20	11.71	1315	61	m
21	A1V	11.94	0.41	0.24	1.00	10.94	862	40	nm
22	G8III	11.95	0.78	1.05	0.80	11.15	555	26	
23	M2III	11.95	0.40	0.41	−0.60	12.55	1841	85	
24	K7V	11.95	0.45	0.84	8.10	3.85	31	2	
25	B8V	11.96	0.36	0.33	−0.25	12.21	1644	76	m?
26	B7Vp	11.98	0.39	0.08	−0.60	12.58	1868	86	OB
27	B7III	12.00	0.47	0.45	−1.50	13.50	2582	119	OB
28	B9V	12.04	0.34	0.05	0.20	11.84	1435	66	m
29	B9V	12.10	0.41	0.36	0.20	11.90	1337	62	m
30	B9V	12.17	0.39	0.23	0.20	11.97	1433	66	m
31	F0Vp	12.21	−0.01	0.00	2.70	9.51	809	37	
32	B9V	12.23	0.37	0.25	0.20	12.03	1508	69	m?
36	A0III	12.43	0.76	0.26	0.00	12.43	1032	48	
42	F6V	12.62	0.30	0.21	3.60	9.02	417	19	
43	M2III	12.65	−0.08	−0.36	−0.60	13.25	5019	231	
10001	B7III	9.78	0.37	0.25	−1.50	11.28	1058	49	m?
10002	K2.5III	9.87	0.65	0.61	0.40	9.47	311	14	
10003	F6V	11.03	0.41	0.02	3.60	7.43	170	8	
10004	M4III	11.03	0.39	−0.14	−0.50	11.53	1158	53	
10005	A5Vp	11.57	0.20	0.12	1.95	9.62	632	29	

Notes. Star # 1: hydrogen lines and metallic spectra are like in a B2 star, He I appears enhanced and Hβ is in emission. Star # 3: hydrogen and metallic lines belong to a spectral type B2; Hβ and Fe II appear in emission. Stars # 4 and # 7: line K of Ca II like in a B9 type; however, H lines and metallic spectra are consistent with a B7 type. Stars # 5 and # 12: line K of Ca II like in a B9 type, but H and He I lines are like in a B8 spectrum. Star # 9: line K of Ca II and He I lines are like in a B5 type, H like in a B6 type and Hβ shows weak emission. Stars # 10 and # 19: He I lines like in a B9 spectrum, line K of Ca II like in a B8 type, Si II and H lines refer to a B3 type, K Ca II and H I as in B3.5, He I 4471 absent, He I 4387 weak emission, Mg I 4481 absent, Si II 4128 stronger in star # 19 than in star # 10. Star # 13: He I and Ca II K lines like in a B9 type, Si II weak and H lines like in a B5 type. Star # 26: He I 4009 and 4026 appear weak. Star # 31: Ca II K line similar to an A0 type, but other spectral features are consistent with a F0V type. Star # 10005: line K of Ca II like in an A3 type and H as in an A5V. Last column: remarks on the membership to NGC 4852 ('m', 'm?', 'nm') or to a farther association ('OB', see Section 5), for stars earlier than A1.

for the solar position) and it is at about 80 pc above the Galactic plane.

The cluster age was derived by looking for the best superposition of solar-metallicity isochrones from Girardi et al. (2000). There is not a previous metal content estimate for this object, but, since it is evidently a young cluster (cf. Fig. 6), we assume that the use of solar isochrones is fully justified. As shown in Fig. 7, isochrones (solid lines) in the V versus $(B-V)$ and V versus $(U-B)$ planes were shifted by eye according to the specific colour excesses and distance moduli obtained above. Since – because of data scatter – there is no single isochrone embracing the entire cluster upper sequence, we prefer to establish an age range within which we are confident with the estimate. The diagrams in Fig. 7 suggest that NGC 4852 is a very young cluster of age ranging from 40 to 60 Myr, far enough from the age limit proposed by Carraro et al. (2005). Since the cluster membership among the brightest stars has been well established

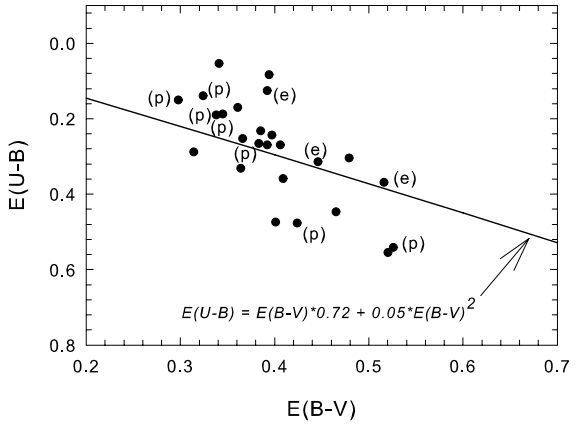

Figure 4. The colour-excess relation from visual colour indices and spectral types. Anomalous stars are labelled as (e) for emission stars and (p) for peculiar stars. The standard extinction law is also shown.

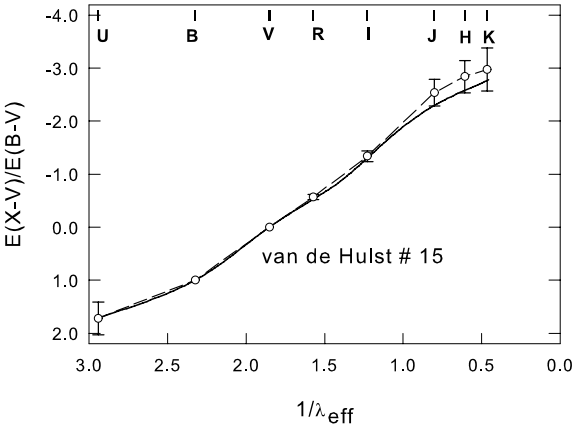

Figure 5. The colour-difference method. Solid line: van der Hulst curve # 15; dashed line: relation we obtained from spectral types and combined visual and infrared indices.

through several colour indices (including $U - B$), we conclude that the cluster is not older than 60 Myr and, equally, not younger than 40 Myr.

When comparing the cluster age derived from the isochrone fitting to the earliest spectral type in NGC 4852, which we set in B6–B7 (see the next section), we recall that the expected hydrogen-burning phase lifetime of a B6–B7 type star is about 100 Myr (Maeder & Meynet 1989), again in contradiction to the limit age proposed previously.

To summarize the photometric findings for NGC 4852, we can say that (i) its mean colour excess $E(B - V)$ is 0.38 ± 0.02 (combining the photometric and spectroscopic results); (ii) its distance is near 1400 pc; and (iii) its age is of the order of 40–60 Myr.

5 SPECTRAL INFORMATION

As described in Section 3, we carried out the spectral classification of 40 stars in NGC 4852, the most extended spectral coverage undertaken on this cluster so far. The results, already presented in Table 5, are discussed in this section.

First, some words on peculiar stars are in order, since it is to be noted that several of our spectra, 10 out of 40, show chemical peculiarities, as specified in the notes to the table. This introduces a difficult problem concerning the precision of the classification in the

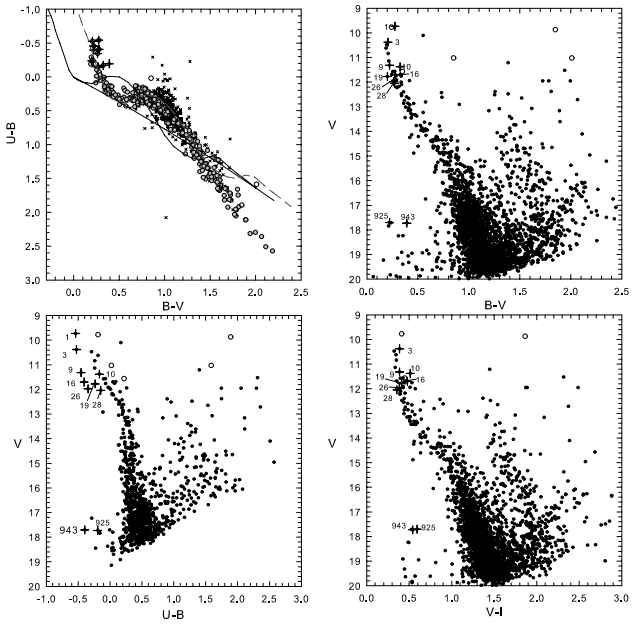

Figure 6. Photometric diagrams of NGC 4852. In the colour–colour diagram (upper left-hand panel), the large grey circles stand for stars brighter than $V = 16$, crosses are stars fainter than 16 and the Schmidt-Kaler (1982) ZAMS is plotted in its normal location (solid line) and shifted to fit the cluster sequence (dashed line). In the other panels, the dots stand for cluster stars and (+) signs represent stars located behind the cluster. Blue stars cited in the text are numbered.

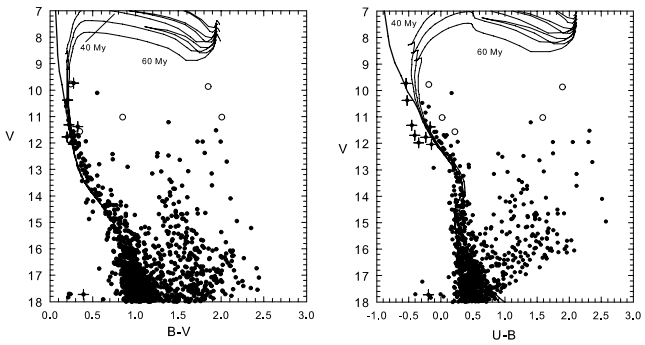

Figure 7. Colour–magnitude diagrams for NGC 4852 where the ZAMS (thick line) and isochrone (thin lines) fittings have been plotted. The isochrones for the age limits estimated for the cluster are labelled. Symbols as in Fig. 6.

MK system and the exact correspondence with the expected colour indices. It is well established that 10–15 per cent of upper main-sequence stars have atmospheres with anomalies in their elemental abundances (Bagnulo 2003) which, in turn, can modify the colours of the stars. According to Jaschek & Jaschek (1987), the phenomena displayed in Bp and Ap stars are very complex, thus making any classification scheme open to criticism: there is a discrepancy between the *UBV* colours of the stars and their spectral types. Other examples of the difficulties in determining precise spectral types of peculiar stars can be seen in Hack (1969) and Shulyak et al. (2009).

Given the high number of stars with chemical peculiarities found in the present survey, we decided, as a general rule, that the spectral classification be performed by analysing H I and He I lines, following the technical procedures suggested by Jaschek & Jaschek (1987). According to the preceding discussion, departures from the

Table 6. Comparison between parameters derived from the spectroscopic analysis (S) and the *Q*-method (Q) for early-type stars in the area of NGC 4852.

Star Id	V	$B-V$	$U-B$	Spectral type (S)	Spectral type (Q)	$E(B-V)$ (S)	$E(B-V)$ (Q)	$E(U-B)$ (S)	$E(U-B)$ (Q)
1	9.73	0.28	−0.54	B2IIIe	B2III	0.52	0.52	0.37	0.36
3	10.38	0.21	−0.53	B2Ve	B2.5	0.45	0.43	0.31	0.30
4	10.47	0.19	−0.29	B7Vp	B6.5	0.32	0.34	0.14	0.24
5	10.62	0.19	−0.19	B8Vp	B8	0.30	0.30	0.15	0.21
6	10.84	0.21	−0.24	B7V	B7	0.34	0.34	0.19	0.24
7	11.14	0.22	−0.24	B7Vp	B7	0.35	0.35	0.19	0.24
9	11.32	0.22	−0.45	B5Ve	B2–B3	0.39	0.43	0.13	0.30
10	11.38	0.33	−0.17	B3Vp	B6–B7	0.53	0.46	0.54	0.32
12	11.57	0.27	−0.07	B8Vp	B8.5	0.38	0.36	0.27	0.25
13	11.58	0.25	−0.10	B5Vp	B8	0.42	0.35	0.48	0.25
14	11.69	0.24	0.09	B9V	B9.5–A0	0.31	0.27	0.29	0.19
15	11.70	0.33	0.04	B9V	B9	0.40	0.39	0.24	0.27
16	11.70	0.28	−0.41	B3V	B3	0.48	0.48	0.30	0.33
17	11.76	0.34	0.07	B9V	B9.5	0.41	0.39	0.27	0.28
18	11.76	0.28	−0.07	B8V	B8.5	0.39	0.37	0.27	0.26
19	11.77	0.20	−0.24	B3Vp	B6.5	0.40	0.33	0.47	0.23
20	11.91	0.29	−0.03	B9V	B8.5–B9	0.36	0.37	0.17	0.26
21	11.94	0.42	0.26	A1V	A0	0.41	0.43	0.24	0.30
25	11.96	0.25	−0.01	B8V	B9	0.36	0.32	0.33	0.22
26	11.98	0.26	−0.35	B7V	B3–B5	0.39	0.44	0.08	0.31
27	12.00	0.34	0.01	B7III	B8–B9	0.47	0.41	0.45	0.29
28	12.04	0.27	−0.15	B9V	B8	0.34	0.38	0.05	0.27
29	12.10	0.34	0.16	B9V	B9–A0	0.41	0.37	0.36	0.26
30	12.17	0.32	0.03	B9V	B9	0.39	0.38	0.23	0.27
32	12.23	0.30	0.05	B9V	B9.5	0.37	0.35	0.25	0.25
10001	9.78	0.24	−0.19	B7III	B7III	0.37	0.36	0.25	0.25

photometric spectral types are likely to happen among several of our stars. To get an appraisal of the possible differences with our spectral classification, we estimated photometric spectral types through the use of the *Q*-method for early-type stars (as in Section 4.2), which provides intrinsic colour indices on the basis of a firmly stated reddening slope, with the caveat that the adoption of a slope of 0.72 for the reddening law has to be taken as just an approximation, given the uncertainties of the MK spectral type and the colour index (see Fig. 4). Some parameters obtained in both ways are compared in Table 6. With the exception of stars # 10, # 13 and # 19, all of them characterized as peculiar, we found no dramatic discrepancy between MK and photometric spectral types. The difference for star # 9, which is of emission type, may be attributed to the colour overcorrection due to the presence of an envelope. Finally, it should not be ignored either that undetected companions, unresolved duplicities or fast rotation may affect colour indices as well.

Bearing this in mind, each star with spectral type was dereddened by assigning intrinsic colour indices following the Schmidt-Kaler (1982) relationship among them, the spectral types and the absolute magnitudes. With this information we computed the spectroscopic parallaxes: colour excesses and individual extinctions, A_V, from the spectral types were obtained and used to calculate intrinsic distance moduli and distances as Table 5 shows in a self-explanatory format.

As for information on the specific stars, searching the literature for previous spectral determinations in the area of NGC 4852 we found the following. Star # 1 (HD 112825, Hen 3-845, CP −59 4639) was classified as B1.5IVe (Feast et al. 1957), but also as B1/2IV/V without emission (Houk & Cowley 1975). Our new analysis yielded that it is a B2IIIe star. The distance of this object (Table 5) implies that it is not a cluster member. Star # 3 (LS 2867, CD −58 4845) was catalogued as an OB$^-$ by Stephenson & Sanduleak (1971). In our spectra, however, this star showed weak Hβ emission, so we classified it as a new emission object with spectral type B2Ve. According to the new data and results given in Table 5, it is not related to the cluster. Star # 4 (CP −58 4630) was previously reported as of spectral type B4(V) by Buscombe (1988); from our new data, it turns out to be a peculiar star that we classified as B7Vp, being a sure member of NGC 4852 according to its distance. Star # 5 (CP −58 4626) was given the spectral type A2(V) by Buscombe (1988); our spectroscopy yielded a spectrum B8Vp. Star # 9 (Wray 15-1039) was classified as an emission star (Wackerling 1970; Stephenson & Sanduleak 1977); we confirmed this emission character and gave it a spectral type B5Ve. This star belongs to a more distant group, according to Table 5. Star # 21 (CP −58 4632) was classified as A0(V) by Buscombe (1988). We assigned it a spectral type A1V and placed it as a foreground star, that is, it has no relation with the cluster. Star # 10001 (HD 112852) was classified as B8/B9II (Houk & Cowley 1975); we set its spectral type as B7III and it is a potential member of NGC 4852. Inspecting Table 5 it is apparent that the evolved stars # 10001 (B7III) and # 36 (A0III) are both at similar distances, but only the first one might be a cluster member, since star # 36 is completely outside the cluster sequence in the main photometric diagrams and its spectral type is too much evolved for the cluster age.

The spectral types allow us to investigate the way in which all these stars are distributed in space; this can be visualized in the plot reddening $E(B-V)$ versus individual star distance (Fig. 8), where for the sake of clarity only blue stars have been labelled with the corresponding spectral type. 11 stars (those marked as 'm' in Table 5), mainly late B-type stars, are probable members of NGC 4852 at a mean distance of 1340 pc with a standard error of

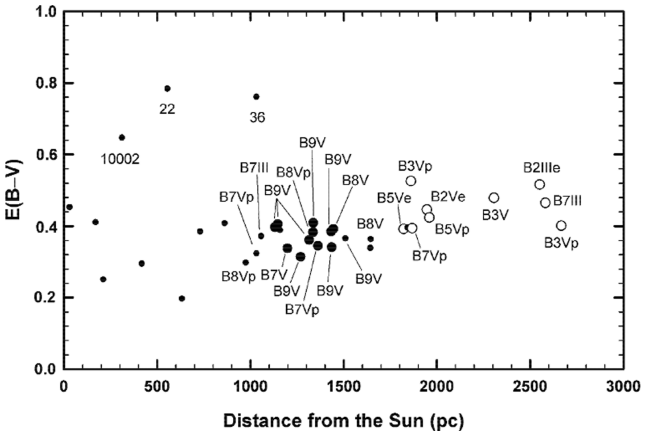

Figure 8. The path of the reddening $E(B-V)$ with the distance from the Sun for each star with spectral type determined in this work. The spectral types of the bluest stars are indicated. The large filled circles represent probable members of NGC 4852 (stars marked as 'm' in Table 5) and the large open circles represent probable members of a farther association (stars marked as 'OB' in the same table).

about 40 pc. There is good agreement between the distance obtained in Section 4.5 and this one from spectral types. Fig. 8 also shows clearly the presence of another (already mentioned) distant star group, composed, in the mean, of earlier B-type stars with distances ranging from 1800 to 2800 pc. This group includes the stars with emission features. In other words, according to our results, the overall picture is the following: NGC 4852 is a star cluster located in front of another, farther, younger, sparse group which may belong to a larger structure that probably includes the clusters NGC 4755 and Loden 694, both at similar distances from the Sun. Our photometric diagrams do not show the presence of other stars of late spectral types together with members of this distant group of B-type stars, which appears alone as if it were formed only by components of an OB association.

Fig. 8 also suggests that the $E(B-V)$ excess smoothly increases after a sudden rise near the solar neighbourhood probably produced by traces of the Coalsack nebula at approximately 200 pc (Hube & Finlay 2007). It must also be pointed out, however, that the fact that stars # 22, # 36 and # 10002 appear with high $E(B-V)$ values, as shown in Fig. 8, may be the result of typical colour uncertainties among evolved red stars.

It is worth noting that 26 out of the 40 stars in the present survey are B-type stars; this is 65 per cent of the sample, a high number indeed. Three of them are of Be type and seven show some spectral peculiarity, but only two peculiar stars appear related to NGC 4852. According to the distances listed in column (8) of Table 5, none of the emission stars belongs to the physical group of NGC 4852; instead, they share a similar location to other B-type stars, thus becoming members of an extensive star formation event behind the cluster. In the last column of Table 5, these stars are flagged as 'OB'.

Finally, we want to note that there are, at the top of the $(U-B)$ versus $(B-V)$ diagram, two blue stars which are extremely faint, stars # 925 and # 943. According to their positions in all the photometric diagrams, these objects are serious candidates to become foreground white dwarfs not related to NGC 4852.

6 CONCLUSIONS

We have performed a photometric and spectroscopic analysis in the region of the open cluster NGC 4852.

We have determined a new distance for this cluster, which is larger than that estimated by Carraro et al. (2005), and have established that the colour excess of NGC 4852 in $(B-V)$ is 0.38. At the same time, our new photometry, which includes most of the brightest stars in the cluster area, has dramatically changed the cluster age previously settled at 200–250 Myr by Carraro et al. (2005), becoming now a very young cluster of less than 60 Myr.

During the course of our spectroscopic survey a new Be-type star has been detected, which raises to three the number of emission objects found in a very small area of the sky. However, the most surprising result is that the distribution of spectral types and distances indicates that the emission-line stars lying in the cluster area do not share any parental relationship with it. In fact, they form part of a more distant group, located at the same distance of some young clusters in the region, like NGC 4755 and Loden 694. They seem to form part of a large structure located behind NGC 4852, extending for more than 1.5 kpc. This situation is compatible with the existence of an OB association and therefore NGC 4852 is located in the innermost part of such a potential star association.

ACKNOWLEDGMENTS

The authors acknowledge the use of the CASLEO CCD and data acquisition system supported under US National Science Foundation grant AST-90-15827 to R. M. Rich. They thank Dr H. O. Levato and Dr R. Gil-Hutton (CASLEO), Dr A. Walker (CTIO), their staff, and the SMARTS Consortium for granting observing time at their respective facilities. EEG, GS and RAV wish to thank the financial support from the IALP (UNLP-CONICET, Argentina) and the PIP No. 1359 from the CONICET. JAA is grateful to Dr M. Salaris and Dr S. Cassisi for financially facilitating his attendance at a meeting where some of these results were first presented. The Digitized Sky Surveys were produced at the Space Telescope Science Institute under US Government grant NAG W-2166. The images of these surveys are based on photographic data obtained using the Oschin Schmidt Telescope on Palomar Mountain and the UK Schmidt Telescope. The plates were processed into the present compressed digital form with the permission of these institutions. Finally, the authors wish to thank the referee, Dr M. Bessell, for his useful comments and suggestions.

REFERENCES

Ahumada J. A., 2008, Mem. Soc. Astron. Ital., 79, 654
Bagnulo S., 2003, in Piskunov N., Weiss W. W., Gray D. F., eds, Proc. IAU Symp. 210, Modelling of Stellar Atmospheres. Astron. Soc. Pac., San Francisco, p. 209
Böhm-Vitense E., Canterna R., 1974, ApJ, 194, 269
Bonatto C., Bica E., Ortolani S., Barbuy B., 2006, A&A, 453, 121
Buscombe W., 1998, 13th General Catalogue of MK Spectral Classification. Northwestern Univ., Evanston
Carraro G., Baume G., Piotto G., Méndez R. A., Schmidtobreik L., 2005, A&A, 436, 527
Cousins A. W. J., 1978, Mon. Not. Astron. Soc. South. Africa, 37, 62
Fabregat J., Torrejón J. M., 2000, A&A, 357, 451
Feast M. W., Thackeray A. D., Wesselink A. J., 1957, Mem. R. Astron. Soc., 68, 1
Giorgi E. E., Solivella G., Vázquez R. A., Orellana R., Núñez J., 2007, New Astron., 12, 461
Girardi L., Bressan A., Bertelli G., Chiosi C., 2000, A&AS, 141, 371
Graham J. A., 1982, PASP, 94, 244
Hack M., 1969, Ap&SS, 5, 403

Houk N., Cowley A. P., 1975, University of Michigan Catalogue of Two-dimensional Spectral Types for the HD Stars. Dept Astron., Univ. Michigan, Ann Arbor
Hube D., Finlay W., 2007, J. R. Astron. Soc. Can., 101, 68
Jaschek C., Jaschek M., 1987, The Classification of Stars. Cambridge Univ. Press, Cambridge
Johnson H. L., 1968, in Middlehurst B. M., Aller L., eds, Nebulae and Interstellar Matter. Univ. Chicago Press, Chicago, p. 167
Kharchenko N. V., Piskunov A. E., Röser S., Shilbach E., Scholz R.-D., 2005, A&A, 438, 1163
Koornneef J., 1983, A&A, 128, 84
Lyngå G., 1987, Lund Catalogue of Open Cluster Data, 5th edn. Centre des Données Stellaires, Strasbourg
McSwain M. V., Gies D. R., 2005, ApJS, 161, 118
Maeder A., Meynet G., 1989, A&A, 210, 155
Mermilliod J.-C., 1976, A&A, 53, 289
Sagar R., Cannon R. D., 1995, A&AS, 111, 75
Salpeter E. E., 1955, ApJ, 121, 161
Scalo J., 1998, in Gilmore G., Howell D., eds, ASP Conf. Ser. Vol. 142, The Stellar Initial Mass Function. Astron. Soc. Pac., San Francisco, p. 201
Schmidt-Kaler Th., 1982, in Schaifers K., Voigt H. H., eds, Landolt-Börnstein, Numerical Data and Functional Relationships in Science and Technology, New Series, Group VI, Vol. 2(b), Star and Star Clusters. Springer-Verlag, Berlin, p. 14
Shulyak D., Ryabchikova T., Mashonkina L., Kochukhov O., 2009, A&A, 499, 879
Skrutskie M. F. et al., 2006, AJ, 131, 1163
Stephenson C. B., Sanduleak N., 1971, Publ. Warner Swasey Obs., 1, No. 1
Stephenson C. B., Sanduleak N., 1977, Publ. Warner Swasey Obs., 2, No. 4
Stetson P. B., 1987, PASP, 99, 181
Stetson P. B., 1990, PASP, 102, 932
Wackerling L. R., 1970, Mem. R. Astron. Soc., 73, 153

SUPPORTING INFORMATION

Additional Supporting Information may be found in the online version of this article:

Table 3. Photometry of NGC 4852.

Please note: Wiley-Blackwell are not responsible for the content or functionality of any supporting materials supplied by the authors. Any queries (other than missing material) should be directed to the corresponding author for the article.

This paper has been typeset from a TEX/LATEX file prepared by the author.